Experimental discrimination between charge 2e/3 top quark and charge 4e/3 exotic quark production scenarios

V.M. Abazov, B. Abbott, M. Abolins, B.S. Acharya, M. Adams, T. Adams, M. Agelou, J.L. Agram, S.H. Ahn, M. Ahsan, et al.

PRL. **98**, 041801 (2007) FERMILAB-PUB-06/278-E

Experimental discrimination between charge $2e/3$ top quark and charge $4e/3$ exotic quark production scenarios

V.M. Abazov,[36] B. Abbott,[76] M. Abolins,[66] B.S. Acharya,[29] M. Adams,[52] T. Adams,[50] M. Agelou,[18] S.H. Ahn,[31] M. Ahsan,[60] G.D. Alexeev,[36] G. Alkhazov,[40] A. Alton,[65] G. Alverson,[64] G.A. Alves,[2] M. Anastasoaie,[35] T. Andeen,[54] S. Anderson,[46] B. Andrieu,[17] M.S. Anzelc,[54] Y. Arnoud,[14] M. Arov,[53] A. Askew,[50] B. Åsman,[41] A.C.S. Assis Jesus,[3] O. Atramentov,[58] C. Autermann,[21] C. Avila,[8] C. Ay,[24] F. Badaud,[13] A. Baden,[62] L. Bagby,[53] B. Baldin,[51] D.V. Bandurin,[60] P. Banerjee,[29] S. Banerjee,[29] E. Barberis,[64] P. Bargassa,[81] P. Baringer,[59] C. Barnes,[44] J. Barreto,[2] J.F. Bartlett,[51] U. Bassler,[17] D. Bauer,[44] A. Bean,[59] M. Begalli,[3] M. Begel,[72] C. Belanger-Champagne,[5] L. Bellantoni,[51] A. Bellavance,[68] J.A. Benitez,[66] S.B. Beri,[27] G. Bernardi,[17] R. Bernhard,[42] L. Berntzon,[15] I. Bertram,[43] M. Besançon,[18] R. Beuselinck,[44] V.A. Bezzubov,[39] P.C. Bhat,[51] V. Bhatnagar,[27] M. Binder,[25] C. Biscarat,[43] K.M. Black,[63] I. Blackler,[44] G. Blazey,[53] F. Blekman,[44] S. Blessing,[50] D. Bloch,[19] K. Bloom,[68] U. Blumenschein,[23] A. Boehnlein,[51] O. Boeriu,[56] T.A. Bolton,[60] G. Borissov,[43] K. Bos,[34] T. Bose,[78] A. Brandt,[79] R. Brock,[66] G. Brooijmans,[71] A. Bross,[51] D. Brown,[79] N.J. Buchanan,[50] D. Buchholz,[54] M. Buehler,[82] V. Buescher,[23] S. Burdin,[51] S. Burke,[46] T.H. Burnett,[83] E. Busato,[17] C.P. Buszello,[44] J.M. Butler,[63] P. Calfayan,[25] S. Calvet,[15] J. Cammin,[72] S. Caron,[34] W. Carvalho,[3] B.C.K. Casey,[78] N.M. Cason,[56] H. Castilla-Valdez,[33] D. Chakraborty,[53] K.M. Chan,[72] A. Chandra,[49] F. Charles,[19] E. Cheu,[46] F. Chevallier,[14] D.K. Cho,[63] S. Choi,[32] B. Choudhary,[28] L. Christofek,[59] D. Claes,[68] B. Clément,[19] C. Clément,[41] Y. Coadou,[5] M. Cooke,[81] W.E. Cooper,[51] D. Coppage,[59] M. Corcoran,[81] M.-C. Cousinou,[15] B. Cox,[45] S. Crépé-Renaudin,[14] D. Cutts,[78] M. Ćwiok,[30] H. da Motta,[2] A. Das,[63] M. Das,[61] B. Davies,[43] G. Davies,[44] G.A. Davis,[54] K. De,[79] P. de Jong,[34] S.J. de Jong,[35] E. De La Cruz-Burelo,[65] C. De Oliveira Martins,[3] J.D. Degenhardt,[65] F. Déliot,[18] M. Demarteau,[51] R. Demina,[72] P. Demine,[18] D. Denisov,[51] S.P. Denisov,[39] S. Desai,[73] H.T. Diehl,[51] M. Diesburg,[51] M. Doidge,[43] A. Dominguez,[68] H. Dong,[73] L.V. Dudko,[38] L. Duflot,[16] S.R. Dugad,[29] D. Duggan,[50] A. Duperrin,[15] J. Dyer,[66] A. Dyshkant,[53] M. Eads,[68] D. Edmunds,[66] T. Edwards,[45] J. Ellison,[49] J. Elmsheuser,[25] V.D. Elvira,[51] S. Eno,[62] P. Ermolov,[38] H. Evans,[55] A. Evdokimov,[37] V.N. Evdokimov,[39] S.N. Fatakia,[63] L. Feligioni,[63] A.V. Ferapontov,[60] T. Ferbel,[72] F. Fiedler,[25] F. Filthaut,[35] W. Fisher,[51] H.E. Fisk,[51] I. Fleck,[23] M. Ford,[45] M. Fortner,[53] H. Fox,[23] S. Fu,[51] S. Fuess,[51] T. Gadfort,[83] C.F. Galea,[35] E. Gallas,[51] E. Galyaev,[56] C. Garcia,[72] A. Garcia-Bellido,[83] J. Gardner,[59] V. Gavrilov,[37] A. Gay,[19] P. Gay,[13] D. Gelé,[19] R. Gelhaus,[49] C.E. Gerber,[52] Y. Gershtein,[50] D. Gillberg,[5] G. Ginther,[72] N. Gollub,[41] B. Gómez,[8] A. Goussiou,[56] P.D. Grannis,[73] H. Greenlee,[51] Z.D. Greenwood,[61] E.M. Gregores,[4] G. Grenier,[20] Ph. Gris,[13] J.-F. Grivaz,[16] S. Grünendahl,[51] M.W. Grünewald,[30] F. Guo,[73] J. Guo,[73] G. Gutierrez,[51] P. Gutierrez,[76] A. Haas,[71] N.J. Hadley,[62] P. Haefner,[25] S. Hagopian,[50] J. Haley,[69] I. Hall,[76] R.E. Hall,[48] L. Han,[7] K. Hanagaki,[51] P. Hansson,[41] K. Harder,[60] A. Harel,[72] R. Harrington,[64] J.M. Hauptman,[58] R. Hauser,[66] J. Hays,[54] T. Hebbeker,[21] D. Hedin,[53] J.G. Hegeman,[34] J.M. Heinmiller,[52] A.P. Heinson,[49] U. Heintz,[63] C. Hensel,[59] K. Herner,[73] G. Hesketh,[64] M.D. Hildreth,[56] R. Hirosky,[82] J.D. Hobbs,[73] B. Hoeneisen,[12] H. Hoeth,[26] M. Hohlfeld,[16] S.J. Hong,[31] R. Hooper,[78] P. Houben,[34] Y. Hu,[73] Z. Hubacek,[10] V. Hynek,[9] I. Iashvili,[70] R. Illingworth,[51] A.S. Ito,[51] S. Jabeen,[63] M. Jaffré,[16] S. Jain,[76] K. Jakobs,[23] C. Jarvis,[62] A. Jenkins,[44] R. Jesik,[44] K. Johns,[46] C. Johnson,[71] M. Johnson,[51] A. Jonckheere,[51] P. Jonsson,[44] A. Juste,[51] D. Käfer,[21] S. Kahn,[74] E. Kajfasz,[15] A.M. Kalinin,[36] J.M. Kalk,[61] J.R. Kalk,[66] S. Kappler,[21] D. Karmanov,[38] J. Kasper,[63] P. Kasper,[51] I. Katsanos,[71] D. Kau,[50] R. Kaur,[27] R. Kehoe,[80] S. Kermiche,[15] N. Khalatyan,[63] A. Khanov,[77] A. Kharchilava,[70] Y.M. Kharzheev,[36] D. Khatidze,[71] H. Kim,[79] T.J. Kim,[31] M.H. Kirby,[35] B. Klima,[51] J.M. Kohli,[27] J.-P. Konrath,[23] M. Kopal,[76] V.M. Korablev,[39] J. Kotcher,[74] B. Kothari,[71] A. Koubarovsky,[38] A.V. Kozelov,[39] J. Kozminski,[66] D. Krop,[55] A. Kryemadhi,[82] T. Kuhl,[24] A. Kumar,[70] S. Kunori,[62] A. Kupco,[11] T. Kurča,[20,*] J. Kvita,[9] S. Lammers,[71] G. Landsberg,[78] J. Lazoflores,[50] A.-C. Le Bihan,[19] P. Lebrun,[20] W.M. Lee,[53] A. Leflat,[38] F. Lehner,[42] V. Lesne,[13] J. Leveque,[46] P. Lewis,[44] J. Li,[79] Q.Z. Li,[51] J.G.R. Lima,[53] D. Lincoln,[51] J. Linnemann,[66] V.V. Lipaev,[39] R. Lipton,[51] Z. Liu,[5] L. Lobo,[44] A. Lobodenko,[40] M. Lokajicek,[11] A. Lounis,[19] P. Love,[43] H.J. Lubatti,[83] M. Lynker,[56] A.L. Lyon,[51] A.K.A. Maciel,[2] R.J. Madaras,[47] P. Mättig,[26] C. Magass,[21] A. Magerkurth,[65] A.-M. Magnan,[14] N. Makovec,[16] P.K. Mal,[56] H.B. Malbouisson,[3] S. Malik,[68] V.L. Malyshev,[36] H.S. Mao,[6] Y. Maravin,[60] M. Martens,[51] R. McCarthy,[73] D. Meder,[24] A. Melnitchouk,[67] A. Mendes,[15] L. Mendoza,[8] M. Merkin,[38] K.W. Merritt,[51] A. Meyer,[21] J. Meyer,[22] M. Michaut,[18] H. Miettinen,[81] T. Millet,[20] J. Mitrevski,[71] J. Molina,[3] N.K. Mondal,[29] J. Monk,[45] R.W. Moore,[5]

T. Moulik,[59] G.S. Muanza,[16] M. Mulders,[51] M. Mulhearn,[71] L. Mundim,[3] Y.D. Mutaf,[73] E. Nagy,[15] M. Naimuddin,[28] M. Narain,[63] N.A. Naumann,[35] H.A. Neal,[65] J.P. Negret,[8] P. Neustroev,[40] C. Noeding,[23] A. Nomerotski,[51] S.F. Novaes,[4] T. Nunnemann,[25] V. O'Dell,[51] D.C. O'Neil,[5] G. Obrant,[40] V. Oguri,[3] N. Oliveira,[3] N. Oshima,[51] R. Otec,[10] G.J. Otero y Garzón,[52] M. Owen,[45] P. Padley,[81] N. Parashar,[57] S.-J. Park,[72] S.K. Park,[31] J. Parsons,[71] R. Partridge,[78] N. Parua,[73] A. Patwa,[74] G. Pawloski,[81] P.M. Perea,[49] E. Perez,[18] K. Peters,[45] P. Pétroff,[16] M. Petteni,[44] R. Piegaia,[1] J. Piper,[66] M.-A. Pleier,[22] P.L.M. Podesta-Lerma,[33] V.M. Podstavkov,[51] Y. Pogorelov,[56] M.-E. Pol,[2] A. Pompoš,[76] B.G. Pope,[66] A.V. Popov,[39] C. Potter,[5] W.L. Prado da Silva,[3] H.B. Prosper,[50] S. Protopopescu,[74] J. Qian,[65] A. Quadt,[22] B. Quinn,[67] M.S. Rangel,[2] K.J. Rani,[29] K. Ranjan,[28] P.N. Ratoff,[43] P. Renkel,[80] S. Reucroft,[64] M. Rijssenbeek,[73] I. Ripp-Baudot,[19] F. Rizatdinova,[77] S. Robinson,[44] R.F. Rodrigues,[3] C. Royon,[18] P. Rubinov,[51] R. Ruchti,[56] V.I. Rud,[38] G. Sajot,[14] A. Sánchez-Hernández,[33] M.P. Sanders,[62] A. Santoro,[3] G. Savage,[51] L. Sawyer,[61] T. Scanlon,[44] D. Schaile,[25] R.D. Schamberger,[73] Y. Scheglov,[40] H. Schellman,[54] P. Schieferdecker,[25] C. Schmitt,[26] C. Schwanenberger,[45] A. Schwartzman,[69] R. Schwienhorst,[66] J. Sekaric,[50] S. Sengupta,[50] H. Severini,[76] E. Shabalina,[52] M. Shamim,[60] V. Shary,[18] A.A. Shchukin,[39] W.D. Shephard,[56] R.K. Shivpuri,[28] D. Shpakov,[51] V. Siccardi,[19] R.A. Sidwell,[60] V. Simak,[10] V. Sirotenko,[51] P. Skubic,[76] P. Slattery,[72] R.P. Smith,[51] G.R. Snow,[68] J. Snow,[75] S. Snyder,[74] S. Söldner-Rembold,[45] X. Song,[53] L. Sonnenschein,[17] A. Sopczak,[43] M. Sosebee,[79] K. Soustruznik,[9] M. Souza,[2] B. Spurlock,[79] J. Stark,[14] J. Steele,[61] V. Stolin,[37] A. Stone,[52] D.A. Stoyanova,[39] J. Strandberg,[41] S. Strandberg,[41] M.A. Strang,[70] M. Strauss,[76] R. Ströhmer,[25] D. Strom,[54] M. Strovink,[47] L. Stutte,[51] S. Sumowidagdo,[50] A. Sznajder,[3] M. Talby,[15] P. Tamburello,[46] W. Taylor,[5] P. Telford,[45] J. Temple,[46] B. Tiller,[25] M. Titov,[23] V.V. Tokmenin,[36] M. Tomoto,[51] T. Toole,[62] I. Torchiani,[23] S. Towers,[43] T. Trefzger,[24] S. Trincaz-Duvoid,[17] D. Tsybychev,[73] B. Tuchming,[18] C. Tully,[69] A.S. Turcot,[45] P.M. Tuts,[71] R. Unalan,[66] L. Uvarov,[40] S. Uvarov,[40] S. Uzunyan,[53] B. Vachon,[5] P.J. van den Berg,[34] R. Van Kooten,[55] W.M. van Leeuwen,[34] N. Varelas,[52] E.W. Varnes,[46] A. Vartapetian,[79] I.A. Vasilyev,[39] M. Vaupel,[26] P. Verdier,[20] L.S. Vertogradov,[36] M. Verzocchi,[51] F. Villeneuve-Seguier,[44] P. Vint,[44] J.-R. Vlimant,[17] E. Von Toerne,[60] M. Voutilainen,[68,†] M. Vreeswijk,[34] H.D. Wahl,[50] L. Wang,[62] M.H.L.S Wang,[51] J. Warchol,[56] G. Watts,[83] M. Wayne,[56] M. Weber,[51] H. Weerts,[66] N. Wermes,[22] M. Wetstein,[62] A. White,[79] D. Wicke,[26] G.W. Wilson,[59] S.J. Wimpenny,[49] M. Wobisch,[51] J. Womersley,[51] D.R. Wood,[64] T.R. Wyatt,[45] Y. Xie,[78] N. Xuan,[56] S. Yacoob,[54] R. Yamada,[51] M. Yan,[62] T. Yasuda,[51] Y.A. Yatsunenko,[36] K. Yip,[74] H.D. Yoo,[78] S.W. Youn,[54] C. Yu,[14] J. Yu,[79] A. Yurkewicz,[73] A. Zatserklyaniy,[53] C. Zeitnitz,[26] D. Zhang,[51] T. Zhao,[83] B. Zhou,[65] J. Zhu,[73] M. Zielinski,[72] D. Zieminska,[55] A. Zieminski,[55] V. Zutshi,[53] and E.G. Zverev[38]

(DØ Collaboration)

[1] *Universidad de Buenos Aires, Buenos Aires, Argentina*
[2] *LAFEX, Centro Brasileiro de Pesquisas Físicas, Rio de Janeiro, Brazil*
[3] *Universidade do Estado do Rio de Janeiro, Rio de Janeiro, Brazil*
[4] *Instituto de Física Teórica, Universidade Estadual Paulista, São Paulo, Brazil*
[5] *University of Alberta, Edmonton, Alberta, Canada, Simon Fraser University, Burnaby, British Columbia, Canada, York University, Toronto, Ontario, Canada, and McGill University, Montreal, Quebec, Canada*
[6] *Institute of High Energy Physics, Beijing, People's Republic of China*
[7] *University of Science and Technology of China, Hefei, People's Republic of China*
[8] *Universidad de los Andes, Bogotá, Colombia*
[9] *Center for Particle Physics, Charles University, Prague, Czech Republic*
[10] *Czech Technical University, Prague, Czech Republic*
[11] *Center for Particle Physics, Institute of Physics, Academy of Sciences of the Czech Republic, Prague, Czech Republic*
[12] *Universidad San Francisco de Quito, Quito, Ecuador*
[13] *Laboratoire de Physique Corpusculaire, IN2P3-CNRS, Université Blaise Pascal, Clermont-Ferrand, France*
[14] *Laboratoire de Physique Subatomique et de Cosmologie, IN2P3-CNRS, Universite de Grenoble 1, Grenoble, France*
[15] *CPPM, IN2P3-CNRS, Université de la Méditerranée, Marseille, France*
[16] *IN2P3-CNRS, Laboratoire de l'Accélérateur Linéaire, Orsay, France*
[17] *LPNHE, IN2P3-CNRS, Universités Paris VI and VII, Paris, France*
[18] *DAPNIA/Service de Physique des Particules, CEA, Saclay, France*
[19] *IPHC, IN2P3-CNRS, Université Louis Pasteur, Strasbourg, France, and Université de Haute Alsace, Mulhouse, France*
[20] *Institut de Physique Nucléaire de Lyon, IN2P3-CNRS, Université Claude Bernard, Villeurbanne, France*
[21] *III. Physikalisches Institut A, RWTH Aachen, Aachen, Germany*
[22] *Physikalisches Institut, Universität Bonn, Bonn, Germany*
[23] *Physikalisches Institut, Universität Freiburg, Freiburg, Germany*
[24] *Institut für Physik, Universität Mainz, Mainz, Germany*
[25] *Ludwig-Maximilians-Universität München, München, Germany*
[26] *Fachbereich Physik, University of Wuppertal, Wuppertal, Germany*

[27] *Panjab University, Chandigarh, India*
[28] *Delhi University, Delhi, India*
[29] *Tata Institute of Fundamental Research, Mumbai, India*
[30] *University College Dublin, Dublin, Ireland*
[31] *Korea Detector Laboratory, Korea University, Seoul, Korea*
[32] *SungKyunKwan University, Suwon, Korea*
[33] *CINVESTAV, Mexico City, Mexico*
[34] *FOM-Institute NIKHEF and University of Amsterdam/NIKHEF, Amsterdam, The Netherlands*
[35] *Radboud University Nijmegen/NIKHEF, Nijmegen, The Netherlands*
[36] *Joint Institute for Nuclear Research, Dubna, Russia*
[37] *Institute for Theoretical and Experimental Physics, Moscow, Russia*
[38] *Moscow State University, Moscow, Russia*
[39] *Institute for High Energy Physics, Protvino, Russia*
[40] *Petersburg Nuclear Physics Institute, St. Petersburg, Russia*
[41] *Lund University, Lund, Sweden, Royal Institute of Technology and Stockholm University, Stockholm, Sweden, and Uppsala University, Uppsala, Sweden*
[42] *Physik Institut der Universität Zürich, Zürich, Switzerland*
[43] *Lancaster University, Lancaster, United Kingdom*
[44] *Imperial College, London, United Kingdom*
[45] *University of Manchester, Manchester, United Kingdom*
[46] *University of Arizona, Tucson, Arizona 85721, USA*
[47] *Lawrence Berkeley National Laboratory and University of California, Berkeley, California 94720, USA*
[48] *California State University, Fresno, California 93740, USA*
[49] *University of California, Riverside, California 92521, USA*
[50] *Florida State University, Tallahassee, Florida 32306, USA*
[51] *Fermi National Accelerator Laboratory, Batavia, Illinois 60510, USA*
[52] *University of Illinois at Chicago, Chicago, Illinois 60607, USA*
[53] *Northern Illinois University, DeKalb, Illinois 60115, USA*
[54] *Northwestern University, Evanston, Illinois 60208, USA*
[55] *Indiana University, Bloomington, Indiana 47405, USA*
[56] *University of Notre Dame, Notre Dame, Indiana 46556, USA*
[57] *Purdue University Calumet, Hammond, Indiana 46323, USA*
[58] *Iowa State University, Ames, Iowa 50011, USA*
[59] *University of Kansas, Lawrence, Kansas 66045, USA*
[60] *Kansas State University, Manhattan, Kansas 66506, USA*
[61] *Louisiana Tech University, Ruston, Louisiana 71272, USA*
[62] *University of Maryland, College Park, Maryland 20742, USA*
[63] *Boston University, Boston, Massachusetts 02215, USA*
[64] *Northeastern University, Boston, Massachusetts 02115, USA*
[65] *University of Michigan, Ann Arbor, Michigan 48109, USA*
[66] *Michigan State University, East Lansing, Michigan 48824, USA*
[67] *University of Mississippi, University, Mississippi 38677, USA*
[68] *University of Nebraska, Lincoln, Nebraska 68588, USA*
[69] *Princeton University, Princeton, New Jersey 08544, USA*
[70] *State University of New York, Buffalo, New York 14260, USA*
[71] *Columbia University, New York, New York 10027, USA*
[72] *University of Rochester, Rochester, New York 14627, USA*
[73] *State University of New York, Stony Brook, New York 11794, USA*
[74] *Brookhaven National Laboratory, Upton, New York 11973, USA*
[75] *Langston University, Langston, Oklahoma 73050, USA*
[76] *University of Oklahoma, Norman, Oklahoma 73019, USA*
[77] *Oklahoma State University, Stillwater, Oklahoma 74078, USA*
[78] *Brown University, Providence, Rhode Island 02912, USA*
[79] *University of Texas, Arlington, Texas 76019, USA*
[80] *Southern Methodist University, Dallas, Texas 75275, USA*
[81] *Rice University, Houston, Texas 77005, USA*
[82] *University of Virginia, Charlottesville, Virginia 22901, USA*
[83] *University of Washington, Seattle, Washington 98195, USA*

(Dated: August 16, 2006)

We present the first experimental discrimination between the $2e/3$ and $4e/3$ top quark electric charge scenarios, using top quark pairs ($t\bar{t}$) produced in $p\bar{p}$ collisions at $\sqrt{s}$=1.96 TeV by the Fermilab Tevatron collider. We use 370 pb^{-1} of data collected by the D0 experiment and select events with

at least one high transverse momentum electron or muon, high transverse energy imbalance, and four or more jets. We discriminate between b- and $\bar{b}$-quark jets by using the charge and momenta of tracks within the jet cones. The data is consistent with the expected electric charge, $|q| = 2e/3$. We exclude, at the 92% C.L., that the sample is solely due to the production of exotic quark pairs $Q\bar{Q}$ with $|q| = 4e/3$. We place an upper limit on the fraction of $Q\bar{Q}$ pairs $\rho < 0.80$ at the 90% C.L.

PACS numbers: 13.85.Rm, 14.65.Ha

The heavy particle discovered by the CDF and D0 collaborations at the Fermilab Tevatron proton-antiproton collider in 1995 [1] is widely recognized to be the top quark. Currently measured properties of the particle are consistent with standard model (SM) expectations for the top quark. However, many of the properties of the particle are still poorly known. In particular, its electric charge, a fundamental quantity characterizing a particle, has not yet been determined.

To date, it is possible to interpret the discovered particle as either a charge $2e/3$ or $-4e/3$ quark. In the published top quark analyses of the CDF and D0 collaborations [2], there is a two-fold ambiguity in pairing the b-quarks and the W bosons in the reaction $p\bar{p} \to t\bar{t} \to W^+W^-b\bar{b}$, and equivalently, in the electric charge assignment of the measured particle. In addition to the SM assignment, $t \to W^+b$, "t"$\to W^-b$ is also conceivable, in which case "t" would actually be an exotic quark, Q, with charge $q = -4e/3$ (charge-conjugate processes are implied). It is possible to fit $Z \to \ell^+\ell^-$ and $Z \to b\bar{b}$ data assuming a top quark mass of $m_t = 270$ GeV and a right-handed b-quark that mixes with the isospin $+1/2$ component of an exotic doublet of charge $-1e/3$ and $-4e/3$ quarks, $(Q1\ , Q4)_R$ [3]. In this scenario, the $-4e/3$ charge quark is the particle discovered at the Tevatron, and the top quark, with mass of 270 GeV, would have so far escaped detection.

In this Letter, we report the first experimental discrimination between the $2e/3$ and $4e/3$ charge scenarios. We also consider the case where the analyzed sample contains an admixture of SM top quarks and exotic quarks and place an upper limit on the exotic quark fraction. Our search strategy assumes each quark decays 100% of the time to a W boson and a b-quark. We use the lepton-plus-jets channel which arises when one W boson decays leptonically and one decays hadronically. The charged leptons (e/μ) originate from a direct W decay or from $W \to \tau \to e/\mu$. We require that the final state have at least two b-quark jets. The data used in this Letter were collected by the D0 experiment from June 2002 through August 2004 and correspond to an integrated luminosity of 370 pb^{-1}.

The D0 detector includes a tracking system, calorimeters, and a muon spectrometer [4]. The tracking system is made up of a silicon microstrip tracker (SMT) and a central fiber tracker, located inside a 2 T superconducting solenoid. The SMT, with a typical strip pitch of 50–80 μm, allows a precise determination of the primary interaction vertex (PV) and an accurate determination of the impact parameter of a track relative to the PV [5]. The tracker design provides efficient charged-particle measurements in the pseudorapidity region $|\eta| < 3$ [6]. The calorimeter consists of a barrel section covering $|\eta| < 1.1$, and two end caps extending to $|\eta| \approx 4.2$. The muon spectrometer encapsulates the calorimeter up to $|\eta| = 2.0$ and consists of three layers of drift chambers and two or three layers of scintillators [7]. A 1.8 T iron toroidal magnet is located outside the innermost layer of the muon detector.

We select data samples in the electron and muon channels by requiring an electron with transverse momentum $p_T > 20$ GeV and $|\eta| < 1.1$, or a muon with $p_T > 20$ GeV and $|\eta| < 2.0$. The leptons are required to be isolated from other particles using calorimeter and tracking information. More details on the lepton identification and trigger requirements are given in Ref. [8]. W boson candidate events are then selected in both channels by requiring missing transverse energy, $\not\!\!E_T$, in excess of 20 GeV due to the neutrino. To remove multijet background, $\not\!\!E_T$ is required to be non-collinear with the lepton direction in the transverse plane. Jets are defined using a cone algorithm [9] with radius $\Delta\mathcal{R} = 0.5$ [10]. These events must be accompanied by four or more jets with $p_T > 15$ GeV and rapidity $|y| < 2.5$. After all the above selection requirements are applied, we have a total of 231 (277) events in the muon (electron) channel.

We use a secondary vertex tagging (SVT) algorithm to reconstruct displaced vertices produced by the decay of B hadrons. Secondary vertices are reconstructed from two or more tracks satisfying: $p_T > 1$ GeV, ≥ 1 hits in the SMT layers, and impact parameter significance $d_{ca}/\sigma_{d_{ca}} > 3.5$. A jet is considered as SVT-tagged if it contains a secondary vertex with a decay length significance $L_{xy}/\sigma_{L_{xy}} > 7$ [11]. The determination of the sample composition relies on b-tagging, c-tagging, and light flavour tagging efficiencies and uses the method described in Ref. [12]. In order to increase the purity of the sample we select only events with two or more SVT-tagged jets. In the selected sample of 21 events with two SVT-tagged jets, the largest (second largest) background is $Wb\bar{b}$ (single top quark [13]) production with a contribution of $\approx 5\%$ ($\approx 1\%$) to the number of selected events.

The top or anti-top quark whose W boson decays leptonically (hadronically) is refered to as the leptonic (hadronic) top and the associated b-quark is denoted b_ℓ (b_h). To compute the top quark charge we need to *i)* de-

cide which of the two SVT-tagged jets are b_ℓ and b_h and *ii)* determine if b_ℓ and b_h are b- or $\bar{b}$-quarks. The detected final state partons in the $t\bar{t}$ candidate events comprise the b_ℓ and b_h quarks, two quarks from the hadronically decaying W boson, and one muon or one electron. The four highest-p_T jets can be assigned to the set of final state quarks according to many permutations and there are at least two ways to assign the SVT-tagged jets to b_ℓ and b_h. For each permutation, the measured four-vectors of the jets and lepton are fitted to the $t\bar{t}$ event hypothesis, taking into account the experimental resolutions and constraining the mass of two W bosons to its measured value and the top quark mass to 175 GeV. We decide which of the SVT-tagged jets are b_ℓ and b_h by selecting the permutation with the highest probability of arising from a $t\bar{t}$ event. Studies on simulated $t\bar{t}$ show that this gives the correct assignment in about 84% of the events.

We measure the absolute value of the top quark charge on each side of the event, given by $Q_1 = |q_\ell + q_{b_\ell}|$ on the leptonic side and $Q_2 = |-q_\ell + q_{b_h}|$ on the hadronic side. The charge of the lepton is indicated by q_ℓ, and q_{b_ℓ} and q_{b_h} are the charges of the SVT-tagged jets on the leptonic and hadronic side of the event. The charges q_{b_ℓ} and q_{b_h} are determined by combining the p_T and charge of the tracks contained within a cone of $\Delta\mathcal{R}$=0.5 around the SVT-tagged jet axis. Based on an optimization using simulated $t\bar{t}$ events generated with ALPGEN [14] and GEANT [15] for a full D0 detector simulation, we define an estimator for jet charge $q_{\rm jet} = \left(\sum_i q_i \cdot p_{T_i}^{0.6}\right) / \left(\sum_i p_{T_i}^{0.6}\right)$ where the subscript i runs over all tracks with $p_T >$ 0.5 GeV and within 0.1 cm of the PV in the direction parallel to the beam axis.

To determine the expected distributions for the top quark charges Q_1 and Q_2, it is crucial to determine the expected distributions for $q_{\rm jet}$ in the case of a b-quark or a $\bar{b}$-quark jet. In ≈5% of the $t\bar{t}$ events, one of the SVT-tagged jets is actually a c-quark jet arising from $W \to c\bar{s}$ (or its charge conjugate). Therefore we also need to determine the expected distribution for $q_{\rm jet}$ in the case of c- and $\bar{c}$-quark jets.

We derive the expected distributions of jet charge from dijet collider data, enhanced in heavy flavor (b and c). We select events with exactly two jets, both SVT-tagged, with $p_T > 15$ GeV and $|y| <$2.5. The method requires that the two jets are of charge conjugate flavors. To ensure this, we enhance $b\bar{b}$ and $c\bar{c}$ produced by flavor creation [16, 17, 18], by requiring the azimuthal distance between the jets to be larger than 3.0 and one jet (designated as j_1) to contain a muon with $p_T > 4$ GeV. We refer to this sample as the "tight dijet sample," to j_1 as the "tag jet" and to the second jet j_2 as the "probe jet."

The fraction of $c\bar{c}$ events in the tight dijet sample is estimated using the distribution of the muon transverse momentum with respect to the tag jet axis ($p_T^{\rm rel}$). We fit the $p_T^{\rm rel}$ distribution with a sum of two $p_T^{\rm rel}$ templates, one for b-quark jets (including both prompt and cascade decays) and one for semi-muonic decays inside c-quark jets. This leads to a fraction x_c of $c\bar{c}$ events of 1^{+2}_{-1}% in the tight dijet sample and since the light flavor tagging efficiency is ≈15 times lower, we also conclude that the fraction of lighter flavor jets is negligible. The muon inside the tag jet comes either i) from a direct B meson decay, ii) a $B \to D$ meson cascade decay, iii) an oscillated neutral B meson, or iv) a direct D meson decay. We find that further contribution from indirect D meson decay can be neglected. Charge flipping processes ii) and iii) lead to a muon of opposite charge to that of the quark initiating the tag jet and therefore of same sign as the quark initiating the probe jet. We find, with PYTHIA [19] simulated events and EVTGEN [20] for heavy flavor decays, that charge flipping processes are $x = (30 \pm 1)$% of the $b\bar{b}$ events in the tight dijet sample. This fraction is experimentally confirmed by studying charge correlation between muons in back-to-back muon-tagged dijet events.

We denote the charge distributions for the probe jet when the muon on the tag side is positive or negative as P_{μ^+} and P_{μ^-}. Similarly we define P_f to be the charge distribution when the jet is of flavor $f = b, \bar{b}, c, \bar{c}$. Given the fractions of $c\bar{c}$ events and of charge flipping processes we can write

$$\begin{aligned} P_{\mu^+} &= 0.69P_b + 0.30P_{\bar{b}} + 0.01P_{\bar{c}} \\ P_{\mu^-} &= 0.30P_b + 0.69P_{\bar{b}} + 0.01P_c. \end{aligned} \quad (1)$$

P_{μ^+} and P_{μ^-} are distributions observed in data and are admixtures of the quark charge distributions. Equations 1 are not sufficient to extract the four probability density functions (p.d.f.'s) P_f. Therefore we define a "loose dijet sample," where j_1 is not required to be SVT-tagged. Using the same techniques as for the tight dijet sample, we find that $x_c = (19 \pm 2)$% and the same fraction of charge flipping processes as for the tight dijet sample. We refer to P'_{μ^+} (P'_{μ^-}) as the observed p.d.f.'s for $q_{\rm jet}$ on the probe jet in the loose dijet sample, when the tag muon is positive (negative). Thus we can write

$$\begin{aligned} P'_{\mu^+} &= 0.567P_b + 0.243P_{\bar{b}} + 0.19P_{\bar{c}} \\ P'_{\mu^-} &= 0.243P_b + 0.567P_{\bar{b}} + 0.19P_c. \end{aligned} \quad (2)$$

We solve Eqs. 1 and 2 to obtain the P_f for b-, $\bar{b}$-, c-, and $\bar{c}$-quark jets.

The P_f's are dependent on the jet p_T, since p_T correlates with track multiplicity in the jet, and on the jet y, since the tracking efficiency is rapidity-dependent. Therefore we must account for the different jet p_T and y spectra between the probe jets of the dijet samples and the b-quark jets in preselected $t\bar{t}$ events. The P_f's obtained above are corrected by weighting the data events to the p_T and y spectra of SVT-tagged jets in $t\bar{t}$ events. Figure 1(a) shows the resulting P_b and $P_{\bar{b}}$.

We derive the expected distributions for Q_1 and Q_2 by applying the assignment procedure between the SVT-

tagged jets and the b_h, b_ℓ quarks on simulated $t\bar{t}$ events using our calculated P_f's. The true flavor f of the SVT-tagged jets is determined from the simulation information. The values of q_{b_h} and q_{b_ℓ} are obtained by randomly sampling the distribution of P_f for the corresponding flavors. About 1% of $t\bar{t}$ candidate events contain a SVT-tagged light-flavor jet. In this case the p.d.f. for $q_{\rm jet}$ is taken from simulation. In the case of a $|q| = 4e/3$ exotic quark, the expected distributions of exotic quark charge are derived by computing $Q_1 = |-q_\ell + q_{b_\ell}|$ and $Q_2 = |q_\ell + q_{b_h}|$, following the same procedure as for the SM top quark. The uncertainty on the mass of the top quark [21] is propagated as a systematic uncertainty.

The expected distributions of Q_1 and Q_2 for the background are obtained by *i)* performing the assignment procedure between SVT-tagged jets and the b_h, b_ℓ quarks on $Wb\bar{b}$ simulated events, *ii)* using the true jet flavors f to sample the corresponding P_f's. The resulting distributions of Q_1 and Q_2 for the background are added to the top charge distributions in the SM and exotic cases. We denote $P_{\rm SM}$ ($P_{\rm ex}$) the p.d.f.'s for Q_1 and Q_2 including the background contributions in the SM (exotic) case.

For 16 of the 21 selected lepton-plus-jet events, the kinematic fit converges and we can assign the SVT-tagged jets to the b_ℓ and b_h quarks, thus providing 32 measurements of the top quark charge. Figure 1(b) shows the 32 observed values of Q_1 and Q_2 overlaid with the SM and exotic charge distributions.

To discriminate between the SM and the exotic hypotheses, we form the ratio of the likelihood of the observed set of charges q_i arising from a SM top quark to the likelihood for the set of q_i arising from the exotic scenario, $\Lambda = [\prod_i P_{\rm SM}(q_i)] \,/\, [\prod_i P_{\rm ex}(q_i)]$. The subscript i runs over all 32 available measurements. The value of the ratio is determined in data and compared with the expected distributions for Λ in the SM and exotic scenarios. We find that the observed set of charges agrees well with those of a SM top quark. The probability of our observation is 7.8% in the case where the selected sample contains only exotic quarks with charge $|q| = 4e/3$, including systematic uncertainties. Thus, we exclude at the 92.2% C.L. that the selected data set is solely composed of an exotic quark with $|q| = 4e/3$. The corresponding expected C.L. is 91.2%. Table I summarizes the dominant systematic uncertainties and their cumulative effect on the C.L.

It is not excluded that the data contain a mixture of two heavy quarks, one with $|q| = 2e/3$ and one with $|q| = 4e/3$. We perform an unbinned maximum likelihood fit to the observed set of q_i in data to determine the fraction ρ of exotic quark pairs. The likelihood of the observed set of q_i can be expressed as a function of ρ by

$$L\,(\rho, q) = \prod_{i=1}^{N_{\rm data}} (1-\rho) P_{\rm SM}(q_i) + \rho P_{\rm ex}\,(q_i) \qquad (3)$$

Systematic	Observed	Expected
Statistical uncertainty only	95.8	95.3
+ Fraction of $c\bar{c}$ events	95.8	95.2
+ Charge-flipping processes	95.7	95.2
+ Weighting w.r.t. p_T and y spectra	94.4	94.1
+ Fraction of flavor creation	93.7	93.4
+ Statistical error on P_f	93.3	93.1
+ Jet energy calibration[a]	92.4	91.8
+ Top quark mass	92.2	91.2

[a]Reference [22].

TABLE I: Expected and observed confidence levels as function of the cumulated systematic uncertainties.

Figure 1(c) shows $-\ln L$ as function of ρ. We fit $\rho = -0.13 \pm 0.66({\rm stat}) \pm 0.11({\rm syst})$, consistent with the SM. Using a Bayesian prior equal to one in the physically allowed region $0 \le \rho \le 1$ and zero otherwise, we obtain $0 \le \rho < 0.52$ at the 68% C.L. and $0 \le \rho < 0.80$ at the 90% C.L.

In summary, we present the first experimental discrimination between the $2e/3$ and $4e/3$ top quark electric charge scenarios. The observed top quark charge is consistent with the SM prediction. The hypothesis that only an exotic quark with charge $|q| = 4e/3$ is produced has been excluded at the 92% C.L. We also place an upper limit of 0.80 at the 90% C.L. on the fraction of exotic quark pairs in the double tagged lepton-plus-jets sample.

We thank the staffs at Fermilab and collaborating institutions, and acknowledge support from the DOE and NSF (USA); CEA and CNRS/IN2P3 (France); FASI, Rosatom and RFBR (Russia); CAPES, CNPq, FAPERJ, FAPESP and FUNDUNESP (Brazil); DAE and DST (India); Colciencias (Colombia); CONACyT (Mexico); KRF and KOSEF (Korea); CONICET and UBACyT (Argentina); FOM (The Netherlands); PPARC (United Kingdom); MSMT (Czech Republic); CRC Program, CFI, NSERC and WestGrid Project (Canada); BMBF and DFG (Germany); SFI (Ireland); The Swedish Research Council (Sweden); Research Corporation; Alexander von Humboldt Foundation; and the Marie Curie Program.

[*] On leave from IEP SAS Kosice, Slovakia.
[†] Visitor from Helsinki Institute of Physics, Helsinki, Finland.

[1] CDF Collaboration, F. Abe *et al.*, Phys. Rev. Lett. **74**, 2626 (1995); D0 Collaboration, S. Abachi *et al.*, Phys. Rev. Lett. **74**, 2632 (1995).
[2] P. C. Bhat, H. Prosper, and S. S. Snyder, Int. J. Mod. Phys. A **13**, 5113 (1998).
[3] D. Chang, W. Chang, and E. Ma, Phys. Rev. D **59**, 091503 (1999); **61**, 037301 (2000); D. Choudhury, T. M. Tait and C. E. Wagner, Phys. Rev. D **65** (2002) 053002.

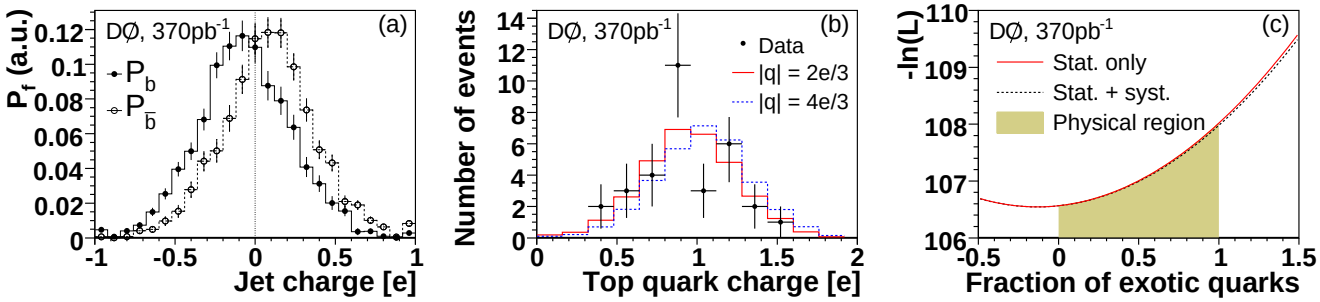

FIG. 1: (a) b and $\bar{b}$ jet charge distributions derived from dijet data, (b) the 32 measured values of the top quark charge compared to the expected distributions in the SM and exotic cases, and (c) likelihood fit of the fraction of exotic quark pairs in the selected data sample.

[4] D0 Collaboration, V. Abazov *et al.*, Nucl. Instrum. Meth. A **565**, 463 (2006).

[5] Impact parameter is defined as the distance of closest approach (d_{ca}) of the track to the primary vertex in the plane transverse to the beamline. Impact parameter significance is defined as $d_{ca}/\sigma_{d_{ca}}$, where $\sigma_{d_{ca}}$ is the uncertainty on d_{ca}.

[6] Rapidity y and pseudorapidity η are defined as functions of the polar angle θ and parameter β as $y(\theta,\beta) = \frac{1}{2}\log(\frac{1+\beta\cos\theta}{1-\beta\cos\theta})$ and $\eta(\theta) = y(\theta,1)$, where β is the ratio of a particle's momentum to its energy.

[7] D0 Collaboration, V. Abazov *et al.*, Nucl. Instrum. Meth. A **552**, 372 (2005).

[8] D0 Collaboration, V. Abazov *et al.*, Phys. Lett. B **626**, 45 (2005).

[9] We use the iterative, seed-based cone algorithm including midpoints, as described on p. 47 in G. C. Blazey *et al.* in *"QCD and Weak Boson Physics in Run II,"* edited by U. Baur, R. K. Ellis, and D. Zeppenfeld, FERMILAB-PUB-00-297 (2000).

[10] $\Delta\mathcal{R}$ is defined as a cone in pseudorapidity- and ϕ-space, $\Delta\mathcal{R} = \sqrt{(\Delta\eta)^2 + (\Delta\phi)^2}$, where ϕ is the azimuthal angle.

[11] Decay length L_{xy} is defined as the distance from the primary to the secondary vertex in the plane transverse to the beamline. Decay length significance is defined as $L_{xy}/\sigma_{L_{xy}}$, where $\sigma_{L_{xy}}$ is the uncertainty on L_{xy}.

[12] D0 Collaboration, V. Abazov *et al.*, Phys. Lett. B **626**, 35 (2005)

[13] A. Puhkov, *et al.*, Report INP-MSU 98-41/542, hep-ph/9908288, 1999.

[14] M. L. Mangano *et al.*, JHEP **07**, 001 (2003).

[15] R. Brun, F. Carminati, CERN Program Library Long Writeup W5013, 1993 (unpublished).

[16] R. D. Field, Phys. Rev. D **65**, 094006 (2002).

[17] CDF Collaboration, D. Acosta *et al.*, Phys. Rev. D **71**, 092001 (2005).

[18] D. A. Wijngaarden, Ph.D. thesis, University of Nijmegen/NIKHEF, FERMILAB-THESIS-2005-14 (2005).

[19] T. Sjöstrand *et al.*, Comp. Phys. Commun. **135**, 238 (2001).

[20] D. J. Lange, Nucl. Instrum. Meth. A **462**, 152 (2001).

[21] TeVatron Electroweak Working Group, hep-ex/0603039.

[22] B. Abbot *et al.*, Nucl. Instrum. Meth. A **424**, 352 (1999).